Revealing the nature of ultra-long period objects with space-based gravitational-wave interferometers

Arthur G. Suvorov,[1] Clara Dehman,[1] and José A. Pons[1]

[1]Departament de Física Aplicada, Universitat d'Alacant, Ap. Correus 99, E-03080 Alacant, Spain

ABSTRACT

A few members of the recently-discovered class of ultra-long period objects have been identified as binaries with white-dwarf primaries. In most cases however, electromagnetic data are inconclusive and isolated magnetars remain a viable candidate. If the pulsation period matches that of the orbit though – as is the case for ILT J1101+5521 and GLEAM-X J0704–37 – several of these elusive radio transients should be gravitational-wave bright in the mHz band. Space-based interferometers could thus be used to provide independent constraints on their nature. We quantify the signal-to-noise ratio for the known systems, assuming they are compact binaries, and show that a few should be detectable with only a few months of data folding. Astrophysical implications for (non-)detections are discussed.

Keywords: gravitational waves, binaries: close, stars: white dwarfs

1. INTRODUCTION

Ultra-long period objects (ULPs) are an elusive class of coherent, radio-pulsating transients with periods of $P \sim$ hours that have thus far evaded classification. Their brightness variations imply compact sources and, given spectral similarities to pulsar emissions, the natural interpretation is that they are slow neutron stars (see Coti Zelati & Borghese 2024, for a discussion). However, this is theoretically challenging to accept as their radio luminosities (L_ν) categorically exceed the implied spindown luminosity, necessitating an alternative power reservoir. While magnetic fields could provide such a battery for magnetar progenitors (Rea et al. 2022; Cooper & Wadiasingh 2024; Suvorov, Dehman & Pons 2025), optical spectroscopy has confirmed that some ULPs are binaries consisting of white dwarfs with M-dwarf companions (WDMDs; Hurley-Walker et al. 2024; de Ruiter et al. 2025). As observational efforts are revealing a sizeable population of ULPs, residing within new portions of the P-$\dot{P}$, L_ν-$L_{\rm X}$, and other parameter spaces, tools to constrain their nature are of astrophysical relevance.

Because pulsations from ILT J1101+5521 and GLEAM-X J0704–37 – confirmed WDMDs – are phase-aligned with their orbital motion (de Ruiter et al. 2025; Rodriguez 2025), this may be the case for other ULPs. Moreover, several of them reside at sub-kpc distances meaning they may be strong sources of gravitational waves (GWs). As eccentricity should be erased before a binary becomes 'ultra-compact' with $P_{\rm orb} \lesssim 1$ hour (Peters 1964), emissions at frequencies of $f_{\rm GW} = 2/P_{\rm orb} \approx 0.6\,{\rm mHz} \times (1\,{\rm hr}/P_{\rm orb})$ ought to dominate the spectrum.

Email: arthur.suvorov@ua.es

Within the next decade, a network of space-based, GW interferometers will become operational, namely the Laser Interferometer Space Antenna (LISA; Amaro-Seoane et al. 2017) plus the two Chinese-led projects Taiji (Luo et al. 2020) and TianQin (Huang et al. 2020), which will be most sensitive in the $\gtrsim$ mHz band. This range is optimal for the detection of ULPs *if* they are WDMDs. Consequently, GW observations can be used to effectively *confirm* or *rule out* binarity in several systems where electromagnetic data are inconclusive.

We show in this Article that, for modest observational windows, at least three sources – CHIME J0630+25, GLEAM-X J162759.5–523504.3, and GPM J1839–10 – are promising candidates for GW detection with large signal-to-noise ratios, SNR $\gg$ 10, with several others being marginal. Some discussion on astrophysical and theoretical implications are also provided.

2. MAGNETIC DWARF BINARY MASSES

Multiband observations of ULPs and the radio-loud binaries Ar Scorpii and AE Aquarii confirm that WDMDs can appear as radio pulsars. In cases where the pulse period is linked to the orbital trajectory, magnetic interactions are likely crucial in mediating the observed emissions. As the companion wades through the magnetosphere of the primary, an electromotive force is generated that drives a 'direct current' with closed field lines serving as the circuit wires (Lai 2012). The formation of such a unipolar inductor instigates energy losses at a rate that depends on the effective resistance in the region linking the orbiters. Because the dissipation rate scales with the square of the near-surface field strength of the primary, it is thought that a precondition for maser-like radio activity in WDMDs is a highly magnetised dwarf ($B_\star \gtrsim 10^8$ G; Melrose 2017; Qu & Zhang 2025).

How a mature white dwarf can harbour a strong field is a matter of active research. However, it may be argued that accretion plays a rôle: Gaia and Sloan Digital Sky Survey (SDSS) data have established that (i) over one third of (semi-detached) cataclysmic variables host a highly-magnetic dwarf (Pala et al. 2020); (ii) observed masses correlate with $B_\star$ (Kawka 2020); and (iii) no young ($\lesssim$ Gyr) detached binaries hosting highly-magnetised dwarfs have been found to date (Belloni & Schreiber 2020). This points towards late-stage dynamo activity, incidentally avoiding problems related to field decay (e.g., Cumming 2002), models of which often invoke rapid rotation. Such features are all naturally explained if the primary underwent accretion epochs involving deposits of mass and angular momentum (Schreiber et al. 2021; Ginzburg et al. 2022).

For these reasons, we assume that primary masses within binary ULPs match those of known magnetic dwarfs, viz. $M_\star \approx (0.87 \pm 0.3) M_\odot$ (see figure 3 in Kawka 2020). This is consistent with orbital solutions for ILT J1101 (de Ruiter et al. 2025) and GX J0704 (Rodriguez 2025). For the companions, broadband photometry and optical spectroscopy indicate $M_{\rm comp} \approx 0.19 M_\odot$ and $M_{\rm comp} \approx 0.32 M_\odot$ in these respective systems. Although observed M dwarf masses span the range $0.1 \lesssim M/M_\odot \lesssim 0.7$ (Cifuentes et al. 2020), we take $M_{\rm comp} = (0.35 \pm 0.2) M_\odot$ to account for possible accretion. These spreads are used to estimate chirp masses,

$$\mathcal{M} = \frac{(M_\star M_{\rm comp})^{3/5}}{(M_\star + M_{\rm comp})^{1/5}} \approx (0.5 \pm 0.2) M_\odot, \quad (1)$$

which set the characteristic GW amplitudes of binaries.

3. ORBITAL GRAVITATIONAL WAVES

The intrinsic GW amplitude of a circular binary reads

$$h_0 \approx 2 \times 10^{-22} \left(\frac{1 \text{ hr}}{P_{\rm orb}}\right)^{2/3} \left(\frac{\mathcal{M}}{0.5 M_\odot}\right)^{5/3} \left(\frac{1 \text{ kpc}}{d}\right), \quad (2)$$

at luminosity distance d. Assuming that the pulse period is that of the orbit, we use the data collated in Table 1 to estimate h_0 from equation (2) for each ULP using the chirp mass spread in expression (1). Notably, the period derivative is moderate in most systems ($\dot{P} \lesssim 10^{-9}$ ss^{-1}; Coti Zelati & Borghese 2024), meaning that GW signals should be essentially monochromatic over $\sim$ yr-long observational windows, T. This allows for an accumulation of signal power over many orbital cycles, $N = T f_{\rm GW} = 2T/P_{\rm orb}$. Averaging over orbital orientations and polarisations, the characteristic strain h_c felt by a detector can thus be estimated through $h_c \approx \sqrt{2N} h_0$ (Finn & Thorne 2000), with value

$$\begin{aligned} h_c \approx 2.1 \times 10^{-20} \left(\frac{1 \text{ hr}}{P_{\rm orb}}\right)^{7/6} \left(\frac{\mathcal{M}}{0.5 M_\odot}\right)^{5/3} \\ \times \left(\frac{T}{0.5 \text{ yr}}\right)^{1/2} \left(\frac{1 \text{ kpc}}{d}\right). \end{aligned} \quad (3)$$

Table 1. Pulsation periods (in descending order) and dispersion-measure (DM) distances for the ULPs considered in this work. Some source names have been shortened.

Source name	Period (s)	Distance (kpc)
CHIME J0630+25[a]	421.4	0.17(8)
GLEAM-X J1627[b]	1091.2	1.3(5)
GPM J1839–10[c]	1318.2	5.7(2.9)
DART/ASKAP J1832[d]	2656.2	4.8(8)
ASKAP J1935[e]	3225.3	4.9(5)
GCRT J1745–3009[f]	4620.7	~ 8
ILT J1101+5521[g]	7531.2	0.50(1.3)
GLEAM-X J0704–34[h]	10496.6	0.4(1)
J1912–4410[i]	14522.2	0.237(5)
ASKAP J1839[j]	23221.7	4.0(1.2)

Notes. [a] Dong et al. (2024) [b] Hurley-Walker et al. (2022) [c] Hurley-Walker et al. (2023) [d] Wang et al. (2024) [e] Caleb et al. (2024) [f] Hyman et al. (2009) [g] de Ruiter et al. (2025) [h] Hurley-Walker et al. (2024); confirmed distance from Gaia photometry (Rodriguez 2025). [i] Pelisoli et al. (2023); UV observations with the Cosmic Origins Spectrograph indicate $M_\star = 0.59(5) M_\odot$ (Pelisoli et al. 2024). [j] Lee et al. (2025).

Using the LISA design specifications from Amaro-Seoane et al. (2017), we adopt the noise power spectral density (S_n) fits from Robson, Cornish & Liu (2019), which include intrinsic noise (from single-link optical metrology and test mass acceleration) as well as Galactic confusion noise from unresolved sources, to estimate ULP detectability. Figure 1 shows characteristic strains h_c from equation (3), as functions of GW frequency, for objects listed in Tab. 1 assuming an observation time of six months. We find that at least two and likely three ULPs (solid symbols) would be readily detectable by LISA (and also by Taiji and TianQin, though not shown) with a few others being marginal under favourable conditions (see Sec. 3.1). As it happens, the most promising candidates are also among the most intriguing.

CHIME J0630. Given its proximity to Earth, insights on local supernovae rates could be gleaned if this source is a neutron star, a position which would be firm if no detection is made shortly after LISA launch. The period would thus correspond to rotation, requiring that some magnetars spindown faster than stipulated by pure dipole braking (e.g. via magnetospheric twist injections; Suvorov, Dehman & Pons 2025). An excess of nearby neutron stars (and magnetars in particular) could also call for revisions to population synthesis models (though see Popov et al. 2003). While a nearby WDMD is not particularly unusual, Tauris (2018) estimates that for SNRs $\gtrsim 100$, $\mathcal{M}$ could be measured to within $\lesssim 1\%$ from which constraints on binary makeup, and possibly even pre-Newtonian effects predicted by some modified theories of gravity (Littenberg & Yunes 2019), follow.
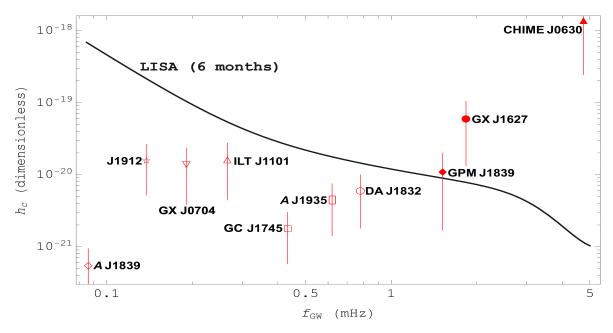
Figure 1. Characteristic strains, equation (3), for ULPs listed in Tab. 1 (see legends) assuming $P = P_{\rm orb}$, $T = 6$ mth, and chirp masses $\mathcal{M} = (0.5 \pm 0.2)\, M_\odot$ from expression (1). Overlaid is the LISA strain curve from Robson, Cornish & Liu (2019).

GX J1627. Discovered in 2018 archival data from the Murchison Widefield Array, this object has since been silent (Hurley-Walker et al. 2022). While Rea et al. (2022) and Lyman et al. (2025) argue that near infrared and spectrophotometric limits disfavour a binary, a high degree of extinction or low inclination could alleviate this tension. As such, a LISA detection would provide valuable information on dust and gas overdensities in the Galaxy. Moreover, the lack of radio reactivation hints at either a choked magnetosphere (e.g. via accretion) or that emissions are beamed inconsistently, either of which holds promise to inform on tight-binary interaction.

GPM J1839. By contrast, this ULP has displayed a high duty cycle ($\sim 25\%$) going back to 1988 (Hurley-Walker et al. 2023). In a neutron-star scenario this points towards aggressive crustal activity despite being old and cold (Cooper & Wadiasingh 2024), which could be used to implicitly constrain magnetar evolution (e.g. Dehman et al. 2020). If confirmed as a WDMD, the fact that the radio luminosity exceeds that of AR Sco by three orders of magnitude indicates that pulsations from binaries involving dwarfs could be highly variable, important to account for in future radio surveys.

3.1. *Signal-to-noise ratios*

In general, a confident detection requires an SNR of at least ~ 10. While detection odds improve for sources with known sky locations, we provide conservative estimates by avoiding complications related to barycentric and other corrections. Borrowing formula (26) from Robson, Cornish & Liu (2019), the orientation- and polarisation-averaged SNR is estimable through

$$\mathrm{SNR} \approx \frac{8\pi^{2/3} G^{5/3} \mathcal{M}^{5/3} f_{\rm GW}^{2/3}}{\sqrt{5}\, c^4 d} \sqrt{\frac{T}{S_n(f_{\rm GW})}} \,, \quad (4)$$

for speed of light c and Newton's constant G. We calculate expression (4) for sources listed in Tab. 1. The results are shown in Table 2 for two scenarios: (i) using the mean value of $\mathcal{M}$ from expression (1) along with best-fit distances, and (ii) an optimistic case where the masses and distances take their upper and lower confidence bounds, respectively. The latter scenario is indicated by bracketed values in the second ($T = 1$ mth) and third ($T = 4$ yr) columns of Tab. 2.

As expected visually from Fig. 1, taking $T \lesssim 4$ yr all but guarantees that CHIME J0630, GX J1627, and GPM J1839 would be identifiable in the LISA data stream. The former two should be visible within a month of first light. While hopes for other ULPs are low, there is some call for optimism for DA J1832 and A J1935 if the components are heavier than average, allowing them to reach significant SNRs when accounting for their sky locations. Because DA J1832 has shown contemporaneous X-ray bursting with radio pulsing (Wang et al. 2024), a magnetar progenitor is favoured over an WDMD (Suvorov, Dehman & Pons 2025); a detection would thus insist on revisions to theoretical models.

4. CONCLUSIONS AND DISCUSSION

ULPs remain mysterious, with some studies favouring isolated neutron stars and others favouring WDMDs (see, e.g., Rea et al. 2022; Coti Zelati & Borghese 2024). We have argued here that *if* ULPs are WDMDs, at least a handful of them should be visible to LISA and its sister spacecraft (Tab. 2). If electromagnetic data remain inconclusive, GW observations could help unveil their nature. Importantly, among the known ULPs, those brightest in the LISA band correspond to objects with uncertain classification (Fig. 1). It is worth comment-

Table 2. SNRs for LISA for the systems listed in Tab. 1 for $T = 1$ mth (middle column) or $T = 4$ yr (right) taking either mean values of the chirp mass, expression 1, and distance or favourable extrema thereof (bracketed values).

Source name	SNR (1 mth; max)	SNR (4 yr; max)
CHIME J0630+25	667 ($> 10^3$)	$> 10^3$ ($> 10^4$)
GLEAM-X J1627	15.9 (48.6)	110 (337)
GPM J1839–10	2.22 (8.53)	15.4 (59.1)
DA J1832	0.42 (0.95)	2.92 (6.59)
ASKAP J1935	0.21 (0.45)	1.47 (3.08)
GCRT J1745–3009	0.04 (0.08)	0.30 (0.57)
ILT J1101+5521	0.14 (0.36)	0.98 (2.49)
GLEAM-X J0704	0.10 (0.19)	0.67 (1.28)
J1912–4410	0.02 (0.05)	0.13 (0.32)
ASKAP J1839	$< 10^{-3}$ ($< 10^{-3}$)	0.002 (0.006)

ing that neutron-star-M-dwarf binaries are not observationally excluded (Hurley-Walker et al. 2024) and could also represent (a subclass of) ULPs. For primaries with $M_\star \approx 1.4 M_\odot$, $\mathcal{M}$ would be larger by $\approx 50\%$ compared to white dwarfs, boosting SNRs by a factor ~ 2.

While some implications of (non-)detections were highlighted in Sec. 3, a wealth of physical processes may operate in ULPs. For instance, linking radio luminosities to electromotive losses implies a minimum strength for the primary's magnetic field. Assuming a maser-like emission mechanism, some systems appear to require GigaGauss strengths (Qu & Zhang 2025). While dynamo action may amplify an internal field (Schreiber et al. 2021), the magnetospheric field may not reflect the interior strength because magnetic burial – a process where field lines are equatorially advected by infalling plasma – will reduce the global dipole moment during accretion while creating strong multipoles (Suvorov & Melatos 2020). Typical accretion rates in tight-binary polars are $\sim 10^{-10} M_\odot$ yr^{-1} (Pala et al. 2020) implying that, for a C/O dwarf with $M_\star \sim 0.8 M_\odot$, the accretion timescale matches that of Ohmic diffusion (τ_Ω) at depths corresponding to densities of $\sim 10^5$ g cm^{-3} where Cumming (2002) estimates $\tau_\Omega \lesssim 1$ Gyr. This suggests a timeline for radio activation post detachment if the interaction zone lies at a polar latitude, with the reverse applying near the equator if magnetic flux is compressed there. Resistive relaxation simulations would help elucidate such interactions and their connections with diamagnetic screening, crystallisation, and convection.

REFERENCES

Amaro-Seoane P. et al., 2017, arXiv:1702.00786
Belloni D., Schreiber M. R., 2020, MNRAS, 492, 1523
Caleb M. et al., 2024, Nature Astronomy, 8, 1159
Cifuentes C. et al., 2020, A&A, 642, A115
Cooper A. J., Wadiasingh Z., 2024, MNRAS, 533, 2133
Coti Zelati F., Borghese A., 2024, arXiv:2412.12763
Cumming A., 2002, MNRAS, 333, 589
de Ruiter I. et al., 2025, Nature Astronomy
Dehman C. et al., 2020, ApJL, 902, L32
Dong F. A. et al., 2024, arXiv:2407.07480
Finn L. S., Thorne K. S., 2000, PhRvD, 62, 124021
Ginzburg S. et al., 2022, MNRAS, 514, 4111
Huang S.-J. et al., 2020, PhRvD, 102, 063021
Hurley-Walker N. et al., 2024, ApJL, 976, L21
Hurley-Walker N. et al., 2023, Nature, 619, 487
Hurley-Walker N. et al., 2022, Nature, 601, 526
Hyman S. D. et al., 2009, ApJ, 696, 280
Kawka A., 2020, IAUS, 357, 60
Lai D., 2012, ApJL, 757, L3
Lee Y. W. J. et al., 2025, Nature Astronomy, 9, 393
Littenberg T. B., Yunes N., 2019, CQG, 36, 095017
Luo Z. et al., 2020, ResPh, 16, 102918
Lyman J. D. et al., 2025, MNRAS, 538, 925
Melrose D. B., 2017, RvMPP, 1, 5
Pala A. F. et al., 2020, MNRAS, 494, 3799
Pelisoli I. et al., 2023, Nature Astronomy, 7, 931
Pelisoli I. et al., 2024, MNRAS, 527, 3826
Peters P. C., 1964, Physical Review, 136, 1224
Popov S. B. et al., 2003, A&A, 406, 111
Qu Y., Zhang B., 2025, ApJ, 981, 34
Rea N. et al., 2022, ApJ, 940, 72
Robson T., Cornish N. J., Liu C., 2019, CQG, 36, 105011
Rodriguez A. C., 2025, A&A, 695, L8
Schreiber M. R. et al., 2021, Nature Astronomy, 5, 648
Suvorov A. G., Dehman C., Pons J., 2025, arXiv:2505.05373
Suvorov A. G., Melatos A., 2020, MNRAS, 499, 3243
Tauris T. M., 2018, PhRvL, 121, 131105
Wang Z. et al., 2024, arXiv:2411.16606